D2.4 Cryosat2 Soil Surface Moisture Algorithm Theoretical Basis Document

v.1.1

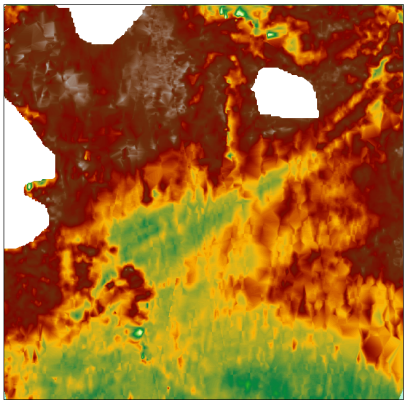

P.A.M. Berry

R. Balmbra

School of Civil Engineering and Geosciences

Newcastle University

United Kingdom

Preparation and Signature List

Name	Company	Signature
P.A.M. Berry	NCL	*Signed on original*
R. Balmbra	NCL	*Signed on original*

Change Log

Version	Date	Changes
1.0	5 June 2014	Created
1.1	18 June 2014	Added sections

Newcastle University
School of Civil Engineering & Geosciences

Table of Contents

Newcastle University
School of Civil Engineering & Geosciences

Figures List

Tables List

1. Introduction

This Algorithm Theoretical Basis Document (ATBD) describes an algorithm used to estimate soil surface moisture from Cryosat2 Level-1b altimeter products. This document identifies the source of input data; outlines the physical principles and mathematical background; justifies this algorithm and then explores its limitations and assumptions.

1.1 Acronyms and Abbreviations List

A list of acronyms and abbreviations is given in Table 1.

Table 1 Acronyms and Abbreviations List

Acronym	Definition
AGC	Automated Gain Control
BES	Berry Expert system
Cryosat2 L1B LRM	Cryosat Level 1B Low Resolution Mode
Cryosat2 L1B SAR	Cryosat Level 1B Synthetic Aperture Radar
CSSME	Cryosat2 Soil Surface Moisture Estimator
dB	Decibels
DMU	De Montfort University
DREAM	DRy EArth Model
ERS	European Remote Sensing Satellite
ESA	European Space Agency
GDR	Geophysical Data Record
LRM	Low Resolution Mode
MGDR	Merged Geophysical Data Record
NEWC	Newcastle University
OCOG	Offset Centre of Gravity
PRF	Pulse Repetition Frequency
RA	Radar Altimeter
RA-2 L1B	Envisat Level 1B Product
SAR	Synthetic Aperture Radar
SGDR	Sensor Geophysical Data Record
SMALT	Soil Moisture from Altimetry
SMOS	Soil Moisture Ocean Salinity satellite
WAP	Altimeter Waveform Product
WF	Waveform

Newcastle University
School of Civil Engineering & Geosciences

2. Algorithm Overview

The algorithm described here is called the Cryosat2 Soil Surface Moisture Estimator (CSSME): it is appropriate for estimating soil surface moisture content from Cryosat2 L1B LRM data, and has been developed using Cryosat2 LRM data. Analysis of the Cryosat2 L1B SAR-LRM transition zone in South Africa (Section 3.2.1.3) indicates that Cryosat2 L1B SAR data should also be appropriate for processing by this algorithm.

2.1 Objective

Soil surface moisture is a key climate variable, with a range of practical applications from informing local climate models (e.g. Drusch, 2007; Crow et al, 2009) to crop analysis (Osborne et al, 2009) and rainfall and runoff predictions (e.g. Brocca et al, 2010: Crow et al, 2009). Because this variable changes spatially and temporally very rapidly, responding to precipitation, surface and sub-surface water flow, the availability of in-situ measurements is limited (Dorigo et al., 2012). There has therefore been sustained interest in the possibility of utilising remote sensing techniques from both passive and active sensors to derive this variable (e.g. Albergel et al., 2009; Doubková et al., 2011; Lacava et al., 2012; Liu et al., 2009; Pathe et al., 2009). The advent of the SMOS mission now provides a dedicated sensor for passive soil surface moisture measurement (Kerr et al., 2012).

An alternative approach has been developed over the past few years, using satellite radar altimetry to measure soil surface moisture in arid and semi-arid terrain, where existing remote sensing methods encounter difficulty (Berry et al., 2013; Berry, et al., 2012; Berry & Carter, 2010; 2011; Bramer & Berry, 2010.). This approach has been progressed into soil surface moisture estimates from the ERS2 and Envisat altimeters in desert and semi-arid terrain under the ESA SMALT project (Berry et al., 2012; SMALT, 2014).

2.2 Instrument Characteristics

CryoSat2 is an altimetry mission launched 8 April 2010 into a near-polar orbit, with the primary objective of studying the Earth's cryosphere. Its mean altitude is 717 km and the orbital inclination gives a latitude limit of 88°, so that almost all the earth's land surfaces are overflown by the satellite. This orbit is not sun-synchronous, and has a repeat period of approximately 369 days, 5344 orbits. This orbit configuration results in a network of closely spaced tracks built up over the earth's surface, but precludes repeat-arc analysis over land surfaces for seasonal change detection. The original mission duration is in negotiation for further extension. Whilst the primary mission is to study the cryosphere, the satellite also retrieves data from most of the earth's surfaces including land.

The primary instrument is the SIRAL altimeter. The instrument has three operating modes. The first, LRM mode, produces data similar to that from previous altimeter missions, and was designed for use over ocean and ice sheet interiors. Here, radar pulses evenly spread at a frequency of 1.97KHz are averaged to produce waveforms at 20Hz. This mode was originally also utilised over most non-cryospheric land surfaces (with the exception of glaciers). The mode of operation is governed by a dynamic mode mask (designed to allow changes in observation mode in response to the dynamically varying sea-ice extent) and this has allowed other changes to the operating mode mask to be made during the mission, resulting in more data over land being acquired in one of the other two modes of operation.

The second mode, SAR mode, combines bursts of coherently transmitted echoes using Synthetic Aperture Radar processing, to reduce the surface footprint in the along-track direction. The primary objective was to enable more precise mapping of ice floes. This mode is now utilized over a significant extent of the earth's land surfaces. The burst mode PRF is 85.7Hz.

The final interferometric mode (SIN mode) is used at the ice sheet margins and over glaciers. Here, the instrument utilizes a second receive only antenna, allowing interferometric processing of the altimeter echoes, to yield more precise slope information. In this algorithm, SAR and LRM data are considered; this document refers to LRM and SAR modes only.

The Cryosat2 SRAL altimeter operation is well outlined in prior reports under LOTUS (e.g. Nielsen et al., 2014) and this is not repeated here.

It is important to note that whilst alterations to the mode mask have allowed areas of the earth's land surfaces originally overflown in LRM mode to be altered to SAR or SIN mode, there is a paucity of SAR mode data over desert surfaces.

2.3 Retrieval Strategy

Determining surface soil moisture from instruments which actively illuminate the earth's surface has primarily been performed using Synthetic Aperture Radar, where the technique is well advanced (e.g. Dobson & Ulaby., 1986 ; Hallikainen et.al., 1985, Engman & Chauhan (1995), Dobson et.al. , 1984;). The principal constraint on this approach is the requirement to populate the theoretical equations with a plethora of information on surface constituents and surface roughness; this requires either detailed information on the surface or a series of assumptions of surface characteristics to be made in order to obtain a solution (e.g. Pathe et al., 2009; Mladenova et al, 2010).

The possibility of utilising satellite radar altimetry to determine soil moisture has been considered for decades (Guzkowska et al., 1990). However, moving from a theoretical possibility to practical application has been problematic, primarily

because similar constraints exist as for SAR soil moisture in the theoretical equations, with the requirement to populate the equations with detailed understanding of surface composition and physical structure. Thus this possibility was not progressed until comparatively recently.

The key to overcoming these constraints is to calculate satellite radar altimeter backscatter by retracking the waveforms, calculating the backscatter, and then combine results from multiple orbits and several satellite missions to yield a backscatter model. This approach is possible because altimeters are nadir-pointing. Screening, editing and reconciling these disparate datasets, and then regressing all data to 'dry earth' conditions then allows the derivation of Dry Earth ModelS (DREAMS) over desert and semi-arid terrain (Berry & Carter, 2011; 2010; Berry et al., 2013; Berry et al., 2012).

Overflying these models with satellite radar altimetry then allows derivation of surface soil moisture for profiles across the landscape underlying the satellite tracks (ibid). Because, even under dry conditions, the earth's physical surface characteristics change rapidly spatially, this approach still does not capture the full extent of surface changes. Additionally, whilst for many surfaces, the backscatter changes with increasing soil moisture, and this allows the derivation of soil surface moisture, salars and smooth surfaces containing mineral salts (such as dry riverbeds) always present bright targets and are typically linear features which are sampled differently at each overpass of the satellite. These features must therefore be excluded from the DREAMS by filtering and masking (ibid). Clearly, any rivers or lakes must also be screened out, as must surrounding terrain that never becomes entirely dry. Rough terrain returns widely varying backscatter values even from spatially adjacent points (such as repeat passes, constrained to a deadband of +/- 1km) and so any significant topographic features must also be excluded from the DREAMs. Using this approach, an ESA funded pilot study has been successfully completed which provides surface soil moisture estimates from ERS2 and Envisat satellite radar altimetry over desert regions (Berry et al., 2012; SMALT; 2014).

3. Algorithm Description

3.1 Theoretical Description

3.1.1 Physics of the Problem

Over ocean, the surface backscatter retrieved by satellite radar altimeters is overwhelmingly dominated by the wave climate and a theoretical model relates the arrival time, noise, backscatter and instrument off-pointing (e.g. Brown, 1977; Challenor, & Srokosz, 1989; Gómez-Enri et al., 2007). With the SRAL instrument, a theoretical model has also been derived (Martin-Puig & Ruffini, 2009) to relate these quantities for SAR waveforms.

Over the earth's land surfaces, theoretical models exist for the response retrieved by Synthetic Aperture Radar, which has been studied for many years. First work in this field showed that, in general, backscatter is strongly dependant on surface roughness, particularly close to nadir, for hh polarisation, (e.g. Ulaby et.al. (1978)). Dobson & Ulaby (1981) examined the relationship between soil tension and backscatter with angle of illumination; however the smallest angle considered was 10 degrees. A series of subsequent studies enhanced the understanding of SAR backscatter interpretation with frequency, angle of illumination and surface characteristics in terms of soil moisture (e.g. Dobson et.al. (1984), Dobson & Ulaby (1986) , Hallikainen et.al (1985), Engman & Chauhan (1995)). One clear concensus from the SAR investigations is that temporal variability is likely to be due to variation in moisture as, in a natural environment, moisture levels may change on much shorter timescales than surface roughness (e.g. Dobson & Ulaby, 1986).

With satellite altimeters, the nadir pointing simplifies one part of the equations; however, the coherent backscattering term then becomes significant. It is possible to model the theoretical parameters to study the dependence of the backscatter, σ_0, upon soil roughness, soil moisture, soil texture and instrument frequency: however, the same detailed requirements for detailed information on target physical characteristics as for SAR have constrained this approach. Very limited research has been published concerning soil surface moisture from satellite radar altimetry prior to the ESA SMALT project (e.g. Guzkowska, 1990; Ridley & Strawbridge (1995)).

Fundamental differences between SAR and radar altimetry must be understood in order to evaluate the applicability of SAR results to altimetry analysis; for example, SAR backscatter values are reported to increase with increasing roughness (Nashashibi et.al. (1996), Oh et.al. (1992)) wheras altimeter backscatter decreases with increasing surface roughness. This is a consequence of the SAR models used by these researchers only considering diffuse scattering, whereas coherent scattering becomes important for the interpretation of satellite radar altimetry data. Side looking SAR only receives the diffuse component as the coherent signal is reflected away from the instrument.

The theoretical approach to soil moisture derivation for satellite radar altimetry thus encounters similar constraints as for SAR; the requirement to populate the equations with detailed information about surface characteristics. This renders this approach unfeasible for large-scale analyses in remote regions.

Fortunately, there is an alternative approach for the interpretation of satellite altimetry, made possible because the instrument is nadir looking. This allows multiple arcs of backscatter observations to be combined, and this, in turn, presents the possibility of creating an empirical model of surface backscatter under dry conditions. This is a complicated process because, even over arid or semi-arid terrain, the earth's surface backscatter changes rapidly spatially, responding to changes in surface roughness and composition. This is the approach taken for the ESA SMALT project (Berry et al., 2012; SMALT, 2014). A brief summary of the data processing approach is included here.

The first step is the derivation of Dry Earth ModelS (DREAMS) for desert areas (ibid). The SMALT DREAM for the Simpson desert is illustrated in Figure 1. This is the full model before masking for geographic feature exclusions.

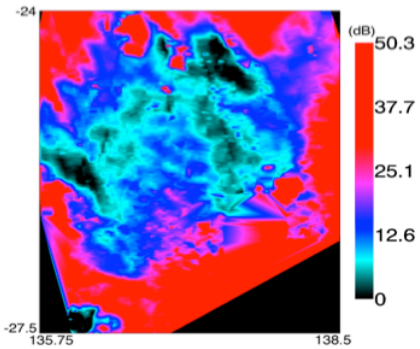

Figure 1 SMALT DREAM of Simpson desert (Soil Moisture from Satellite Radar Altimetry (SMALT) (from Berry et al., 2012)

These models can still contain signals from paleo-hydrology features, inland water, sand dunes and terrain discontinuities e.g. mountains. These must be excluded by additional masking before a DREAM can be used. At this stage, the DREAM is confronted with actual data. For the ESA SMALT project, utilising ERS2 (WAP) and Envisat (SGDR) data with a 35 day repeat cycle (ibid) an analysis of one year of cross-calibrated recalculated backscatter from each mission was used to analyse DREAM performance, and identify high frequency spatial anomalies not fully captured by the DREAM ibid). Most commonly, these arise where a dry river bed or small salar is present. Figure 2 shows a typical ERS2 analysis for one repeat track over the Simpson desert DREAM. Here, one cycle (shown in turquoise) has elevated backscatter difference across the DREAM, indicating that the surface had appreciable moisture content at the time of the ERS2 overpass. Looking in more detail at these

data, Figure 3 shows two subsets of the profiles where short wavelength features are apparent in some or all tracks. These are parts of the profiles where the DREAM does not fully capture the high frequency backscatter changes on the surface. The +/- 1km across-track orbit constraint means that the overpasses are sampling the high frequency features differently in each cycle. Such effects will contaminate the soil moisture estimates, and so these regions are excluded from the SMALT processing chain.

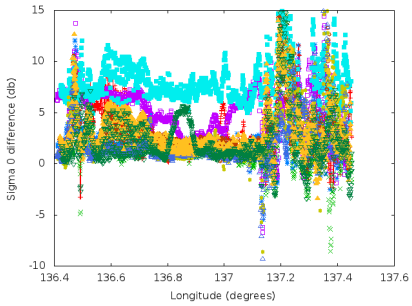

Figure 2 ERS2 Repeat Arc Analysis for one track - difference from Simpson DREAM

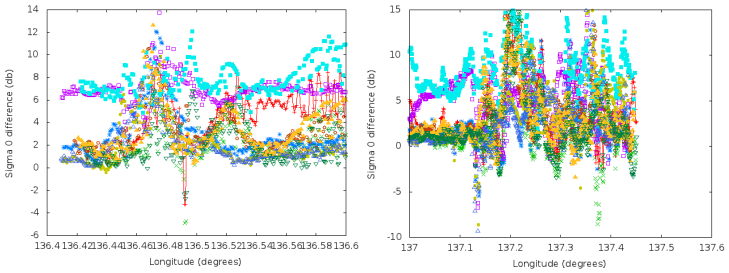

Figure 3 ERS2 Exclusions over Simpson DREAM for track in Figure 2

The effect of this additional filtering can be assessed by looking at the distribution of the differences between the cross-calibrated ERS2 backscatter and the DREAM for each track for each cycle before and after filtering (Figure 4).

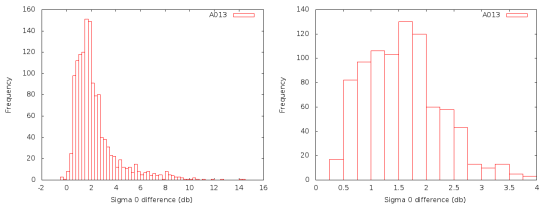

Figure 4 Histograms before and after exclusions for track in Figure 6 for ERS2 Cycle 13

It is clear that the filtering has been effective in removing residual contamination. Whilst this approach cannot be taken for Cryosat2 data, it is strongly recommended that this part of the DREAM evaluation strategy is carried out for Sentinel3, in addition to utilising a minimum of 1 year of repeat arc data to over-populate the

DREAM along the Sentinal3 repeat arcs. Further years of data should then be used over all DREAMs to screen out residual contamination from paleo-hydrology/abrupt changes in surface constituents/ roughness/ terrain, prior to soil moisture estimation.

At this stage, the data are averaged along-track to obtain a stable estimate. The extent of averaging was made variable for SMALT, in order to optimise the soil moisture data produced over each DREAM. For illustration, the processing chain used in SMALT is shown in Figure 5 (Berry et al., 2012).

The lack of multiple repeat arc data for Cryosat2 means that extensive further DREAM testing will be required using a full repeat cycle of Cryosat2 data to fully evaluate the model and add additional masking and filtering. However, a similar scheme in outline to that shown in Figure 5 can be utilised in principle for soil moisture determination from Cryosat2. In detail, however, the lack of repeat arc data means that substantive additional data screening and editing are required, in addition to a more complex procedure to cross-calibrate Cryosat2 backscatter to the DREAM models.

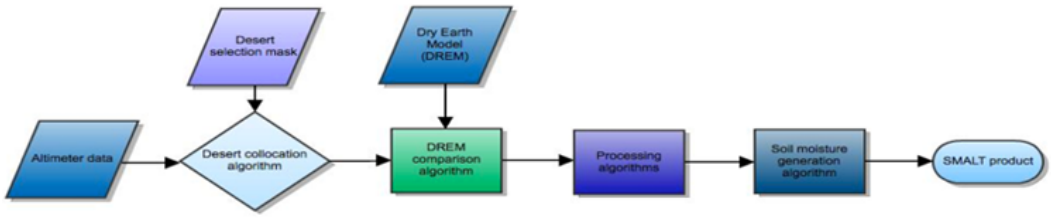

Figure 5 SMALT Processing Diagram (from Berry et al., 2012)

Utilising this approach, soil surface moisture estimates can then be calculated.

For ERS2, soil moisture estimates derived utilising a research scheme similar to that in Figure 3 have been compared with external data to validate the soil surface moisture derivation (Berry & Carter 2010; 2011; Berry et al., 2012) . One primary source for validation has been the Australian AussieGRASS model (AussieGRASS 2014). A typical result for the Simpson desert validation is shown in Figure 6 for clarity.

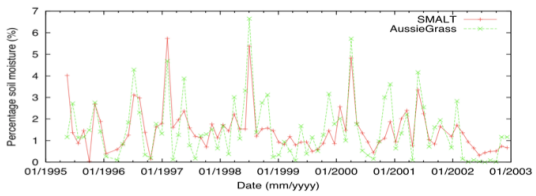

Figure 6 Simpson desert ERS2 SMALT soil moisture estimates with AussieGRASS model (from Berry et al, 2012)

3.1.2 Re-crafting DREAMS for Cryosat2

Cryosat2 does not have a short repeat orbit, and so the techniques utilised to optimise soil moisture retrieval from Cryosat2 altimeter backscatter have to be modified. The DREAMs must be significantly enhanced to the point where they can be utilised without repeat arc information, and the screening and editing methodology must be enhanced to identify and then exclude short wavelength model errors as well as short wavelength features in the Cryosat2 backscatter profiles not well captured by the DREAMs.

Figure 7 Simpson desert ERS1 Crossover Locations for DREAMcrafting

The first stage of this work has been to assess the desert characteristics and select best DREAMS for re-crafting for use without repeat arc filtering.

The Simpson desert (Fig. 7) was selected as this has been the primary calibration site for land backscatter across multiple altimeter missions for soil moisture derivation.

The Tenere desert within the vast expanse of the Sahara was chosen as the DREAM performance was stable across the model when confronted with multi-mission satellite altimeter backscatter data. Thus the Tenere is a good choice for non-repeat missions.

Whilst the Kalahari desert represents a very difficult and challenging target for a DREAM, even with a repeat arc mission, the environmental importance of this region necessitates its inclusion. However, it has taken much new research to re-craft the model to a level where non-repeat data could be utilised. On a practical note, the fact that this desert experiences significant rainfall for several months each year means that non-zero soil moisture should be sampled by Cryosat2 in any year of operation.

The DREAM models selected underwent four stages of model re-crafting; sample results are illustrated here for the ERS1-GM dataset. The final models utilise multi-mission datasets from ERS1, ERS2, Envisat and Jason1. Example results are shown for the Simpson desert in Figures 8 & 9. Whilst the rapid short wavelength variation

in desert backscatter precludes using crossover adjustment to create a DREAM, the aggregated statistics still give a measure of model enhancements.

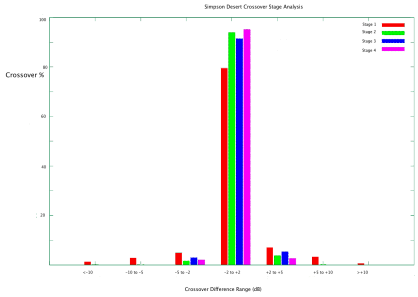

Figure 8 Analysis during DREAM crafting for Simpson desert (Berry, Dowson & Carter 2013

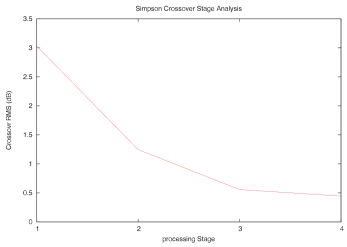

Figure 9 Simpson RMS reduction during DREAM crafting (ibid)

Figure 8 shows the gradual improvement in crossover difference histograms during model crafting for the Simpson desert; Figure 9 shows the corresponding crossover RMS reduction. The final model for the Simpson desert is illustrated in Figure 10, masked to exclude the irregular dunefields where backscatter characteristics change too rapidly.

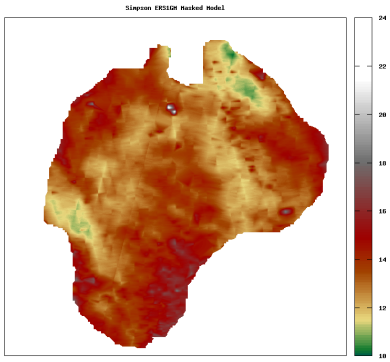

Figure 10 Masked DREAM of Simpson Desert after Enhancements

3.1.3 Mathematical Description of the Algorithm

The processing is in two parts. The first part processes sequential records from one pass over a DREAM. The second analyses the sequence to produce soil moisture estimates from this pass.

Stage 1 Individual Record Processing

The flow diagram for Stage 1 processing is shown in Figure 11.

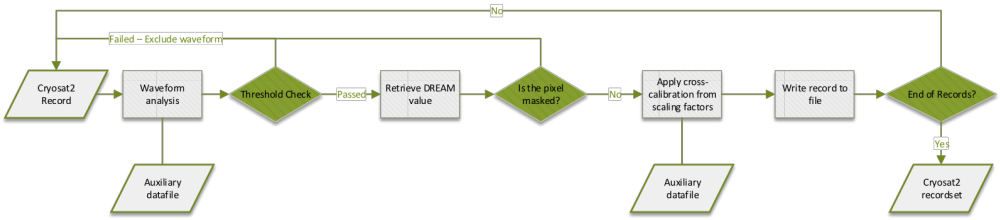

Figure 11 Flow chart for Stage 1 Processing

The processing stages are outlined here.

Waveform Analysis

Input record from the Cryosat2 L1B product; check waveform for significant power present and to exclude waveforms where the leading edge is missing. Check all error flags and exclude flagged records from further

analysis.

Analyse Cryosat2 waveform using the OCOG parameterisation:
Calculate waveform width (W) and corrected amplitude (A).

$$Amplitude = \sqrt{\frac{\sum_{i=1+n_l}^{n_u-1} P_i^4}{\sum_{i=1+n_l}^{n_u-1} P_i^2}}$$

$$Width = \frac{\left(\sum_{i=1+n_l}^{n_u-1} P_i^2\right)^2}{\sum_{i=1+n_l}^{n_u-1} P_i^4}$$

Where

i is bin number

p_i is waveform power in bin i

n_l and n_u are the lower and upper aliasing exclusion limits

Note that waveform power is assumed transformed to microwatts prior to calculation.

This approach is noise-tolerant and gives an adequate representation of backscatter for this purpose for waveforms from diffusely reflecting desert surfaces. When wet, these surfaces become brighter and again, OCOG gives an adequate corrected amplitude estimate for this purpose as the filtering excludes very bright returns, although this algorithm is not generally recommended for land height retracking.

Compare with empirically determined lower and upper thresholds for amplitude A (A_L and A_U) and width W (W_L and W_U) and exclude waveforms outside these ranges. The purpose of this filter is to exclude echoes returned from bright targets, either salar or surface water, very low power returns, and, as far as possible, echoes from rough/sloping surfaces remaining within the masked DREAMs.

Retrieve DREAM Value

Calculate σ_{0_CRY} using equation of form:

$\sigma_{0\_CRY} = 10\ LOG_{10}(Amplitude/Sig\_A) + Sig\_B$

where Sig_A and Sig_B are constants in the IPF2 configuration file (Cryosat Product Handbook, 2012).

Using latitude and longitude of record, retrieve DREAM value for overflown pixel. If pixel value set to Masked then exclude record from further analysis.

Apply Cross-Calibration

Apply pre-determined cross-calibration scaling factors from auxiliary datafile to re-reference σ_{0_CRY} to the DREAM backscatter range (DREAMS are created with an offset to all values to keep the DREAM backscatter always positive). An auxiliary datafile is therefore utilised to adjust the mission recalculated backscatter to the correct range for each DREAM.

$\sigma_{0CRY\_ADJ} = \sigma_{0CRY}$ + Offset

Calculate difference for each altimeter point from corresponding DREAM pixel.

$\sigma_{0diff} = \sigma_{0CRY\_ADJ} - \sigma_{0DREAM}$

Error trap. Where σ_{diff} >LIMIT2, exclude point from further analysis. This test is required to allow for the contingency that the full variation in surface characteristics may not be successfully captured by the model. For Sentinel3, repeat arc analysis and model masking can be utilised, at which point this test may become redundant.

Stage 2 Record Sequence Processing

At this stage records form one pass over the DREAM are analysed. The processing scheme is shown in Fig. 12, and the steps are described below.

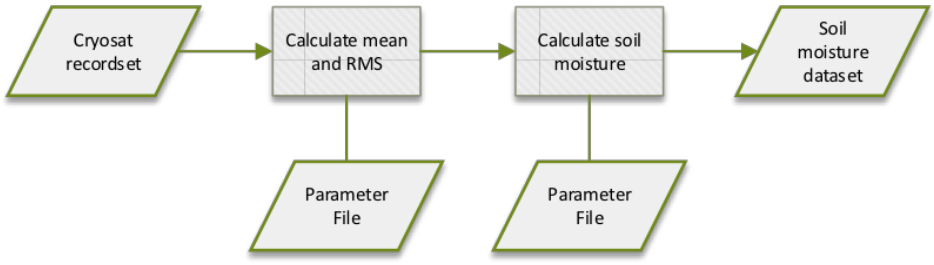

Figure 12 Flow Chart for Stage 2 Processing

Calculate Mean and RMS

Where σ_{diff} < LIMIT1, pass values to the averaging algorithm.

Read parameter file for number of points to be averaged along-track. Create mean value σ_{mean} and RMS σ_{rms}.

Initial settings for this average will be for the whole pass over a DREAM, yielding a track_average soil moisture estimate from the processing chain. However, it may be possible to increase the spatial resolution; this will be determined after the processing scheme has been confronted with multiple passes of Cryosat2 data over each desert. Thus the configuration allows for multiple soil moisture estimates to be created along one pass. It is also noted that the necessary extent of averaging may vary between DREAMS. The Simpson DREAM with previous altimeter missions allowed the highest product spatial resolution (SMALT, 2014), and the Kalahari desert the lowest (ibid).

Calculate Soil Moisture

Reading parameter values from parameter file, transform to first soil surface moisture estimate using equation of form:

$Soil\_Moisture = M1*\sigma_{diff} + M2$

This equation is appropriate for soil moisture less than approximately 5% (saturated surface soil moisture is approximately 8%).. This equation may be replaced by a more sophisticated equation after testing over a range of soil surface moisture conditions. The reason for taking this approach is that to utilize the more complicated equation and have it perform satisfactorily requires sampling the Cryosat2 backscatter over the DREAMS through a range of surface soil moisture conditions. Because the terrain is arid or semi-arid, multiple years of data may need to be amassed before the equation empirically determined constants can be sufficiently well determined. For Sentinel3 it is expected that this tuning can be completed more rapidly, as the presence of repeat arc data allows more direct comparisons within a constrained ribbon of ground track: one year of data has been sufficient to form a baseline with prior altimeter missions with repeat cycles of 10-35 days.

3.1.4 Parameter Description

Key parameters used in this processing are listed in Table 2.

Table 2 Parameter summary table

Symbol	Descriptive Name	I/O	Origin
σ_{0CRY}	Sigma0 value recalculated from waveform amplitude using scaling factors	Internal	Calculated in processing
Sig_A	Scaling parameter for backscatter calculation	Input	From IPF2 configuration file
Sig_B	Scaling parameter	Input	From IPF2 configuration file
P_i	Waveform power in bin i	Input	Input from Cryosat2 L1B datafile and rescaled to microwatts
i	Bin number	Input	Assigned at Cryosat2 L1B data read-in
A	Waveform Amplitude	Internal	Calculated in processing
W	Waveform Width	Internal	Calculated in processing
σ_{0CRY_ADJ}	σ_{0CRY} scaled for DREAM comparison	Internal	
σ_{0diff}	Sigma0 difference from DREAM	Internal	Calculated in processing
σ_{0DREAM}	Sigma0 value from DREAM pixel	Internal	Input from DREAM
σ_{mean}	Mean Sigma0	Internal	
σ_{rms}	RMS of mean Sigma0	Internal	May be output to inform error estimates
Soil_Moisture	Percentage soil moisture estimate	Output	Calculated in processing

Parameters from the Auxiliary Datafile input datafile of empirical values required for calculation are shown in Table 3. Note that these values may be different for each desert; thus a separate set of values will be associated with each desert DREAM.

Table 3 Parameter File List

Name	Units	Comment
A_L	Microwatts	Empirically determined amplitude lower limit
A_U	Microwatts	Empirically determined amplitude upper limit
W_L	Bins	Empirically determined width lower limit
W_U	Bins	Empirically determined width upper limit
Masked	dB	Exotic unit set to exclusion value in DREAM
Offset	dB	Exotic unit set for each DREAM
Limit1	dB	Exotic unit set for each DREAM
Limit2	dB	Exotic unit set for each DREAM
M1	None	Scaling factor 1
M2	None	Scaling factor 2
N_points	None	Number of points used to create σ_{mean}

Values are read separately for each desert to allow cross-calibration to each model, and to allow the potential to change exclusion criteria according to model behaviour.

3.1.5 Error Budget Estimates

Forming error estimates arising from the DREAM is difficult without repeat arcs. It is possible to utilise the DREAM statistics to estimate the uncertainty in the model for each DREAM. σ_0 must be cross-calibrated to each model before soil moisture can be derived, and necessary smoothing, and spike exclusions performed. Whilst initial estimates can be made using σ_{rms}, this will only capture the along-track variation compared to the DREAM. For a more complete analysis, large amounts of Cryosat2 data must be processed to challenge both the DREAMs and the processing algorithms.

3.2 Practical Considerations

This algorithm is appropriate for desert and semi-arid areas. The accuracy of the soil moisture estimate is critically dependent on the quality of each DREAM. Whilst the algorithm has been tested using Cryosat2 LRM data (see section 3.2.1) the S.

Africa cross-comparison work indicates that SAR data should also be appropriate for this algorithm.

3.2.1 Calibration and Validation

In order to utilise this approach, cross-calibration is required for each desert between the recalculated σ_0 estimate and the DREAM.

3.2.1.1 Simpson DREAM First Assessment with Cryosat2 data

Calculating the backscatter from Cryosat2 LRM data and then comparing with the DREAM over the Simpson desert allowed a first cross-calibration with the DREAM to be carried out. Further more extensive cross-calibration with a minimum of 6 months of data will be required to complete this activity. A typical example track is shown in Figure 13, with a vertical offset to aid comparison. Here, the DREAM has been masked where dunefields are present. The requirement for this is clear from Figure 13; the backscatter values from Cryosat2 are seen to oscillate widely outside the DREAM model region. In contrast, the DREAM model region backscatter is stable and presents a good comparison. However, additional masking is advisable at the LHS of the plot, where the DREAM values are changing quite rapidly, and more variability is seen in the Cryosat2 backscatter values.

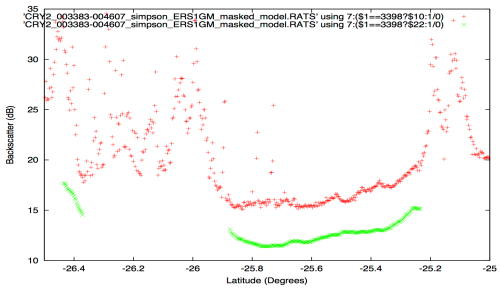

Figure 13 Cryosat2 example track across Simpson DREAM (Cryosat2 sigma0 red, DREAM green; vertical offset for clarity)

3.2.1.2 Tenere DREAM First Assessment with Cryosat2 data

The masked model re-crafted for the Tenere desert Cryosat2 work is shown in Figure 14.

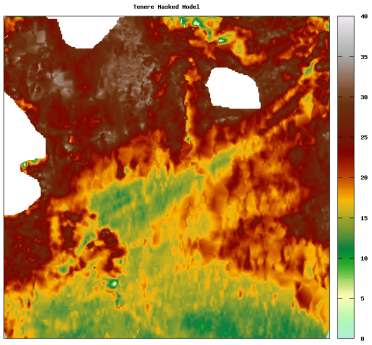

Figure 14 Tenere masked model re-crafted for Cryosat2

Here, a rugged terrain region is excluded within the DREAM (white enclosed area) and further regions have been excluded in the LHS of the region. This region is more variable in its surface characteristics than the Simpson desert, but the DREAM exhibits stable behaviour and only intermittent exclusions are found when tested with ERS2 backscatter. Accordingly, the enhanced model was tested with Cryosat2 recalculated backscatter, with very promising results for the cross-calibration. A typical profile is shown in Figure 15.

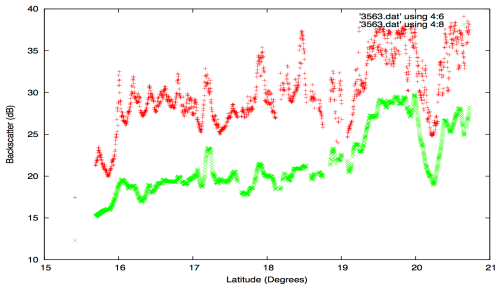

Figure 15 Cryosat2 track 9red) across Tenere DREAM (green) plotted with offset for clarity

Here, more short wavelength variability in Cryosat2 backscatter is seen than for the Simpson desert; this is expected, as the surface structures change more rapidly for the Tenere desert. However, quite good agreement is noted between the DREAM and the Cryosat2 recalculated backscatter. Somewhat higher variability is observed; this is expected, as the highest frequency terrain variations are not completely captured by the DREAM. Along-track filtering and averaging procedures are thus required to produce stable soil moisture estimates.

3.2.1.3 Kalahari DREAM First Assessment with Cryosat2 data

The Kalahari presents an extremely challenging target. Even with repeat arc data to aid in model masking, deriving soil moisture estimates from the Kalahari desert is problematic (REF SMALT). The re-crafted and masked model for the Kalahari DREAM for Cryosat2 data is shown in Figure 16.

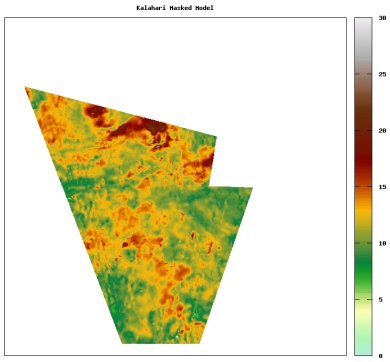

Figure 16 Kalahari re-crafted and masked model for Cryosat2

This desert presents an extremely challenging target, because the presence of water for a few months each year makes the surface characteristics extremely variable, with many high wavelength terrain roughness and surface constituent variations. However, because this is such an important region for soil moisture determination, for a variety of scientific applications, this area was included.

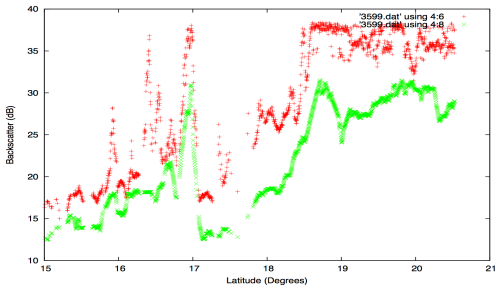

Figure 17 Example comparison Cryosat2 re-calculated backscatter (red) with Kalahari DREAM (green) plotted with offset for clarity

An example profile from Cryosat2 recalculated backscatter over the masked Kalahari model is shown in Figure 17. The more variable nature of the surface response is clearly seen in the DREAM model backscatter, and is echoed in the Cryosat2 profile. However, clear correlation is seen between the DREAM and the Cryosat2 data, which

is extremely encouraging, and indicates that this desert region can be utilised for Cryosat2 soil moisture measurement. It is noted that additional screening and filtering will be required in the processing chain, with the relevant parameters determined after extensive testing and soil moisture calculation with a minimum of 1 year of Cryosat2 data. Whilst the model has been re-crafted, the current model masking is derived from that required for the SMALT project (SMALT, 2014); it is anticipated that further model masking may be required for Cryosat2 soil moisture derivation.

3.2.1.3 South Africa LRM to SAR comparison

One remaining issue must be addressed: as all DREAM areas are overflown by Cryosat2 in LRM mode, an analysis is required to determine whether the schema in this document may be applicable to Cryosat2 SAR mode waveforms. Over South Africa, both SAR and LRM data are retrieved in adjacent areas of sparsely vegetated terrain (Figure 18) ; however this terrain is too variable both in terrain variability and water storage capacity (lakes, rivers, irrigation) to create a DREAM. However, this does provide an area to compare LRM mode data to SAR mode data.

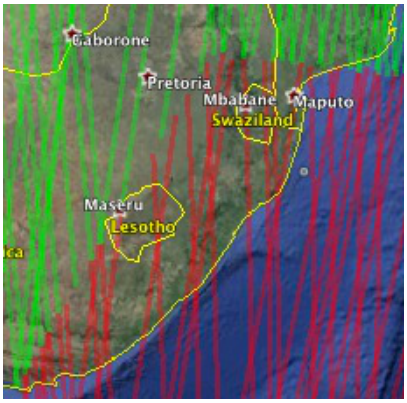

Figure 18 Cryosat2 LRM and SAR areas over South Africa

The actual data subset for this analysis is shown in Figure 19.

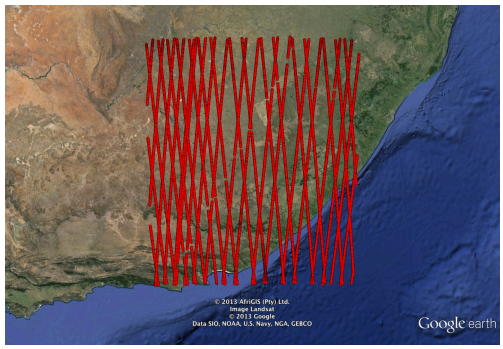

Figure 19 Cryosat2 tracks over South Africa for 3 months of data, one dot per waveform

A waveform type analysis was carried out for all echoes shown in Figure 19. Typical results are given in Table 5 for 4 tracks. Ocean echoes contribute to the water echo total; however a significant number of quasi-specular returns are found, indicating the presence of bright targets on the surface. Analysis of the distribution confirms that these are distributed across the region, in some cases identifiable with rivers/salars, whilst others appear to be associated with areas where agriculture is evident. There is a high proportion of slope-affected echoes, again understandable given the terrain variation. The dominant category for both LRM and SAR echoes in this region is complex multi-target responses; these cannot reliably be used for soil moisture estimation.

Table 4 Waveform analysis for four tracks in South Africa semi-arid region in Figure 19

TRACK ID	A mode 0	B mode 1	C mode 0	D mode 1	
Broad echoes	22	3	3	8	
Water/salar echoes	128	83	107	272	
Slope affected echoes	123	7	38	18	
Complex multi-target	584	493	308	682	
Flat patch	1	59	19	163	

The backscatter for both LRM and SAR modes was calculated, and the cross-calibration offsets were added from the DREAM analysis. This causes all backscatter estimates to be biased high, but makes inter-comparison of the data shown in these figures with those from the DREAM analysis more transparent. Figure 20 shows a typical track containing both LRM and SAR mode data over the area in Figure 19. High variability is apparent across this profile in both LRM and SAR modes, a result entirely consistent with observed backscatter behaviour in the DREAM analysis outside the DREAM model areas. Figure 21 shows the retracked height profile. Figure 22 shows a further backscatter profile across this region and includes a portion of ocean data for comparison (note that these values have also been offset using the DREAM comparison offsets, hence the high values over ocean). Figure 23 shows the corresponding height profile.

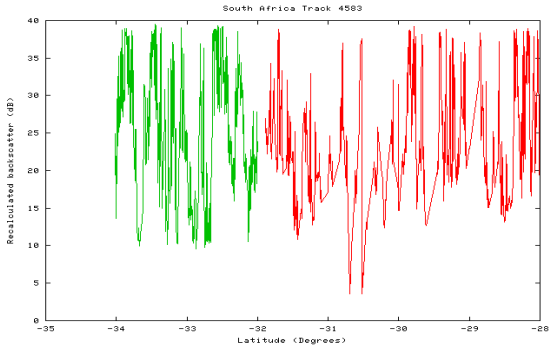

Figure 20 Cryosat2 track showing recalculated backscatter (cross-calibrated to DREAM model range) for orbit 4583 showing LRM backscatter (green) and SAR backscatter (red)

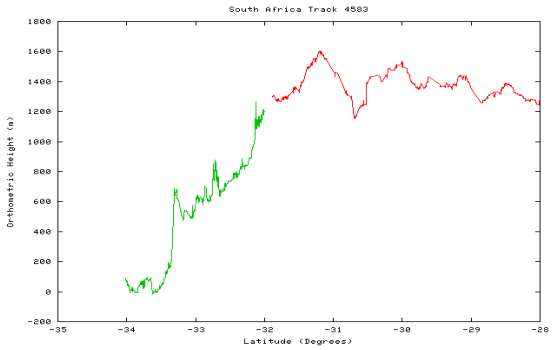

Figure 21 Cryosat2 track showing orthometric height across region for orbit 4583 (LRM green, SAR red

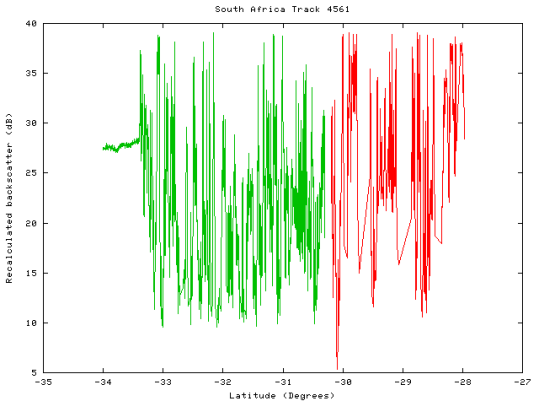

Figure 22 Cryosat2 track showing recalculated backscatter (cross-calibrated to DREAM model range) for orbit 4561 showing LRM backscatter (green) and SAR backscatter (red)

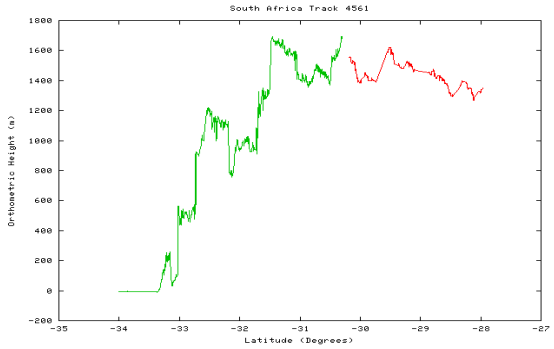

Figure 23 Cryosat2 Orthometric Height for orbit 4561 across region (LRM green, SAR red)

Analysis of three months of Cryosat2 data over this region did not find any part of the area where backscatter behaviour was sufficiently stable and predictable to attempt to recover estimates of soil moisture from Cryosat2 even if a DREAM could be created. This approach was therefore discontinued. However, this research shows that the behaviour of Cryosat2 SAR mode and LRM mode recalculated backscatter to be comprehensible in terms of surface characteristics; it is thus concluded that calculating soil moisture utilising SAR mode waveforms is viable.

3.2.2 Quality Control and Diagnostics

It is assumed that all relevant error flags on the Cryosat2 L1B input data are read and error flagged points are excluded from processing. The empirical tests on permitted sigma0 range for each DREAM are set to exclude non-viable sigma0 estimates.

3.2.4 Output Product

Each output product will consist of a series of estimates of soil surface moisture under one satellite track for one DREAM, with an associated mean time value, and start and stop latitude and longitude coordinates for the track segment included in each estimate. The spatial separation of these estimates is configurable within the processing in order to obtain the optimal spatial resolution allowed by the DREAMs. Essential output parameters for each record are listed in Table 4.

Table 5 Output Essential Parameter List

Parameter	Unit
Segment start Longitude	Decimal degrees
Segment start Latitude	Decimal degrees
Segment End Longitude	Decimal degrees
Segment End Latitude	Decimal degrees
Year	Year
Month	Month
Day	Day
Fraction of day at centre of track segment	Decimal day
Soil moisture mean estimate	Percentage soil moisture
Number of points in estimate	none
Altimeter mode of operation	Textfield

4. Assumptions and Limitations

4.1 Assumptions

The following assumptions were made in the design of the CSME.

1. Altimeter waveforms are available without error flags. Flagged data are excluded.

2. Altimeter waveforms have already been pre-processed, and units transformed to microwatts. Null waveforms and incompletely captured waveforms (critically those where the leading edge is not captured) are excluded.

3. A DREAM model is available, already masked for exclusion criteria, together with its parameters file.

4. It is assumed on the basis of the backscatter behaviour of Cryosat2 LRM data and the cross-comparison with Cryosat2 SAR data over S. Africa that the performance of Cryosat2 SAR mode data will be suitable for this algorithm. However, significant amounts of Cryosat2 SAR data will be required to calculate Parameter File List values (Table 3).

4.2 Limitations

The current version of this algorithm may have the following limitations.

1. DREAM availability constrains operation of this algorithm to arid or semi-arid terrain

2. This algorithm has been developed utilising Cryosat2 LRM data as a test set, as no SAR data are currently available over DREAM areas. Cross-comparison of SAR and LRM data reported here indicates that the sigma0 performance is comparable and that this approach will also be appropriate for SAR waveforms. Noisy backscatter is noted outside the DREAM model areas, even in extremely dry terrain.

5. References

Albergel et al. 2009: An evaluation of ASCAT surface soil moisture products with in-situ observations in Southwestern France. Hydrol. Earth Syst. Sci., 13, 115–124

AussieGRASS 2014: http://www.longpaddock.qld.gov.au/about/researchprojects/aussiegrass/

Berry, P.A.M., Smith, R.G., Witheridge, S.R., Salloway, M,K, Benveniste, J. , 2012. Soil Moisture from Satellite Radar ALTimetry (SMALT). EGU poster.

Berry, P.A.M., Dowson, M., Smith, R.G., Benveniste, J., 2012. Soil Moisture From Satellite Radar Altimetry (SMALT). Proceedings of the ESA Living Planet Symposium 2012.

Berry, P.A.M., Carter, J.O., 2011. Altimeter derived Soil Moisture Determination – Global Scope and Validation. IAHS 'red book' for IUGG 2011.

Berry, P A. M. & Carter, J.O., 2010. Cross Calibration of SMOS Soil Moisture Measurements with Satellite Radar Altimetry Estimates and In-Situ Data. Proceedings of ESA Living Planet Symposium, ISBN 978-92-9221-250-6.

Berry, P.A.M., Dowson, M. & Carter, J.O., 2013. Surface Soil Moisture From Multi-Mission Satellite Radar Altimetry. Proceedings of ESA Living Planet 2013, In Press.

Bramer, S.M.S. & Berry, P.A.M. 2010. Soil Surface Moisture From EnviSat RA-2: From Modelling Towards Implementation. P205-212, International Association of Geodesy Symposia, Vol. 135, ISBN: 978-3-642-10633-0.

L. Brocca et al.,2010. Improving runoff prediction through the assimilation of the ASCAT soil moisture product, Hydrology and Earth System Sciences Discussions, vol. 7 (4), no. 4, pp. 4113-4144, 2010.

Brown, G.S., 1977. The Average Impulse Response of a Rough Surface and Its Applications, IEEE Trans. Antennas Propag., vol. AP-25, pp. 67-74, Jan.1977.

Challenor, P. G., and M. A. Srokosz, 1989. The extraction of geophysical parameters from radar altimeter return from a non-linear sea surface. *Mathematics in Remote Sensing,* S. R. Brooks, Ed., Clarendon Press, 257–268.

W. T. Crow, G. J. Huffman, R. Bindlish, and T. J. Jackson, 2009. Improving satellite-based rainfall accumulation estimates using spaceborne surface soil moisture retrievals, Journal of Hydrometeorology, vol. 10, no. 1, pp. 199-212, 2009.

Cryosat Product Handbook, 2012: CryoSat-PHB-17apr2012.pdf .

Dobson M. & Ulaby F., 1981. Microwave Backscatter Dependance on Surface Roughness, Soil Moisture, and Soil Texture: Part III - Soil Tension IEEE Transactions on Geoscience and Remote Sensing, V GE-19, No. 1, 1981.

Dobson M., Kouyate F. & Ulaby F., 1984. A Reexamination of Soil Textural Effects on Microwave Emission and Backscattering. IEEE Transactions on Geoscience and Remote Sensing, V GE-22, No. 6, 1984

Dobson M. & Ulaby F., 1986. Active Microwave Soil Moisture Research, IEEE Transactions on Geoscience and Remote Sensing, V GE-24, N0. 1, 1986

Dorigo, W. A., Wagner, W., Hohensinn, R., Hahn, S., Paulik, C., Xaver, A., Gruber, A., Drusch, M., Mecklenburg ,S., van Oevelen, P., Robock, A . and Jackson, T. , 2012. The International Soil Moisture Network: a data hosting facility for global in situ soil moisture measurements. Hydrol. Earth Syst. Sci., 15, 1675–1698, 2011.

M. Doubková, A. I. J. M. Van Dijk, G. Blöschl, D. Sabel, and W. Wagner, 2011. Evaluation of predicted soil moisture retrieval error from C-Band SAR by comparison against soil moisture estimates over Australia, Remote Sensing of Environment, 2011.

Drusch, M. , 2007. Initializing numerical weather prediction models with satellite-derived surface soil moisture: Data assimilation experiments with ECMWF's Integrated Forecast System and the TMI soil moisture data set. *Journal of Geophysical Research 112: doi: 10.1029/2006JD007478. issn: 0148-0227*

Engman E. & Chauhan N. , 1995. Status of Microwave Soil Moisture Measurements with Remote Sensing. Remote Sensing of the Environment. v. 51, pp. 189-198, 1995

J. Gómez-Enri, C. P. Gommenginger, M. A. Srokosz, And P. G. Challenor, 2007. Measuring Global Ocean Wave Skewness by Retracking RA-2 *Envisat* Waveforms. 1102 Journ. Atm. & Oc.Tech. Volume 24, pp1102 – 1116. *Laboratory for Satellite Oceanography, National Oceanography Centre, Southampton, United Kingdom*

Guzkowska, M.A.J., Rapley, C.G., Ridley, J.K., Cudlip, W., Birkett, C.M. and Scott, R.F. ,1990. Developments in inland water and landaltimetry, ESA Contract, CR-7839/88/F/FL.

Hallikainen M., Ulaby F., Dobson M. El-Rays M. & Wu L. ,1985. Microwave Dielectric Behaviour of Wet Soil Part 1 Empirical Models and Experimental Observations. IEEE Transactions on Geoscience and Remote Sensing V GE-23 N.1 1985

Kerr, Y. H., P. Waldteufel, J. P. Wigneron, J. M. Martinuzzi, J. Font and M. Berger, 2001. Soil moisture retrieval from space: The Soil Moisture and Ocean Salinity (SMOS) mission. IEEE Transactions on Geoscience and Remote Sensing 39(8): 1729-1735

Kerr, Y. H., P. Waldteufel, P. Richaume, J. P. Wigneron, P. Ferrazzoli, A. Mahmoodi, A. Al Bitar, F. Cabot, C. Gruhier, S. E. Juglea, D. Leroux, A. Mialon and S. Delwart, 2012. "The SMOS Soil Moisture Retrieval Algorithm." IEEE Transactions on Geoscience and Remote Sensing 50(5): 1384-1403.).

Lacava, T., Brocca, L., Faruolo, M., Matgen, P., Moramarco, T., Pergola, N., Tramutoli, V., 2012. A multi-sensor (SMOS, AMSR-E and ASCAT) satellite-based soil moisture products inter-comparison. Proceedings 2012 IEEE International Geoscience and Remote Sensing Symposium (IGARSS), 1135-1138, doi:10.1109/IGARSS.2012.6351348.

Liu, Y. Y., Van Dijk, A. I. J. M., De Jeu, R. A. M. and Holmes, T. R. H., 2009. An analysis of spatiotemporal variations of soil and vegetation moisture from a 29-year satellite-derived data set over mainland Australia, Water Resources Research, vol. 45, no. 7, p. art. no. W07405, 2009.

Martin-Puig, C. & Ruffini, G., 2009. SAR Altimeter Retracker Performance Bound over Water Surfaces. IGARSS (5) ,pp 449-452.

Mladenova, I., Lakshmi, V., Walker, J. P., Panciera,R., Wagner, W. and Doubkova, M., 2010. Validation of the ASAR global monitoring mode soil moisture product using the NAFE'05 data set, IEEE Transactions on Geoscience and Remote Sensing, vol. 48, no. 6, pp. 2498-2508, 2010.

Nashashibi A., Ulaby F. & Sarabandi K., 1996. Measurement and Modeling of the Millimeter-Wave Backscatter Response of Soil Surfaces IEEE Transactions on Geoscience and Remote Sensing V 34 No.2

Nielsen, K. et al., 2014. State of the Art Review of SAR mode over Land. LOTUS Report, D2.1.

Oh Y., Sarabandi K. & Ulaby F., 1992. An Emperical Model and an Inversion Technique for Radar Scattering from Bare Soil Surfaces. IEEE Transactions on Geoscience and Remote Sensing V 30 No. 2 1992.

Osborne, T., Slingo,J., Lawrence, D. and Wheeler, T., 2009. Examining the interaction of growing crops with local climate using a coupled crop-climate model, Journal of Climate, vol. 22, no. 6, pp. 1393-1411, 2009.

Pathe, C., Wagner, W., Sabel,, D. Doubkova, M. and Basara, J., 2009. Using ENVISAT ASAR Global Mode Data for Surface Soil Moisture Retrieval Over Oklahoma, USA. IEEE Transactions on Geoscience and Remote Sensing, vol. 47, no. 2, pp. 468-480, 2009.

Ridley, J., Strawbridge, F., Card R. and Phillips H., 1996. Radar Backscatter Characteristics of a Desert Surface, Remote Sensing of the Environment, Vol 57, No 2, pp63-78.

SMALT, 2014. http://tethys.eaprs.cse.dmu.ac.uk/SMALT/

Ulaby F., Batlivala P. & Dobson M., 1978. Microwave Backscatter Dependence on Surface Roughness, Soil Moisture, and Soil Texture: Part 1 Bare Soil. IEEE Transactions on Geoscience Electronics, V GE-16, No. 4, 1978